Safety Augmentation for Volitional Human Locomotion via Lower-Limb Exoskeletons: A Case Study

Miao Yu, *Student Member, IEEE*, Qin Lin, *Member, IEEE*, and Ge Lv, *Member, IEEE*

***Abstract*—User safety is a crucial factor to consider when designing control paradigms for lower-limb exoskeletons. Existing control paradigms mainly focus on providing assistance for human users under stable walking conditions, ignoring situations that human users may lose their balance due to external perturbations during locomotion. In this letter, we propose a safety framework for lower-limb exoskeletons to augment safety for volitional human motion based on Control Barrier Functions. The safety indicators are defined as the human's center of mass and swing foot position lying within self-selected ranges. Instead of enforcing reference trajectories, we incorporate human inputs and preferences in a two-layer quadratic program structure based on Control Barrier Functions to generate assistance for ensuring safety. Simulation results on a human wearing an exoskeleton demonstrate that the proposed control paradigm can generate assistance to assist human users in maintaining balance while undergoing gait perturbations and recovering from initial unsafe postures.**

***Index Terms*—Safety Augmentation, Exoskeleton, Control Barrier Functions, Nonlinear Disturbance Observer.**

I. Introduction

FALLS and fall-related injuries bring a significant health problem for adults of all ages. In the year of 2018, 27.5% of adults aged 65 or above reported at least one fall in the past year, and 10.2% reported a fall-related injury [1]. One in ten U.S. adults reports falling each year, and among all age groups, falls can cause serious injury and are the second leading cause of traumatic brain injury–related deaths [2]. Various devices have been developed to improve balance and reduce the risk of falling for humans during walking. Traditional ambulatory-assistive devices such as canes and walkers are commonly adopted among elderly individuals to improve walking balance and reduce the risk of potential falls [3]. While these devices can provide assistance to restore balance, critical barriers still exist in promoting these devices to the general population. Canes and walkers require constant grasping by their users, thus limit the user's overall mobility. Prior studies also indicate that such devices can potentially jeopardize walking stability [3]. Other ambulatory devices, which are often used in clinics, also lack adaptability to daily human activities.

M. Yu and G. Lv are with the Department of Mechanical Engineering, Clemson University, Clemson, SC 29634, USA (e-mail: {myu2, glv}@clemson.edu). Q. Lin is with the Department of Engineering Technology, University of Houston, Houston, TX 77004, USA (e-mail: qlin21@central.uh.edu). Corresponding author: Ge Lv.

This work is partially supported by the National Science Foundation under grant 2301543. Any opinions, findings, and conclusions or recommendations expressed in this material are those of the authors and do not necessarily reflect the views of the National Science Foundation.

Emerging powered lower-limb exoskeletons have addressed the issue of mobility and demonstrated great potential in assisting their human users across activities [4], such as bearing the weight of extra loads [5], reducing energy expenditure [6], and restoring normative gait kinematics [7]. In addition to providing assistance, control paradigms were also developed to regain balance. For instance, capture point theory was used to design balance control strategies under large perturbations [8] for humanoids and to correct unsafe leaning motion of humans to avoid a potential fall [9]. A "help when needed", time-dependent control paradigm was developed to enable exoskeletons to assist balance recovery [10]. Zhu et al. designed a control strategy based on slip recoverability regions to assist human users to regain balance with unexpected foot slips [11].

While there is extensive existing literature on exoskeleton balance control, most of the proposed methods do not adapt well to various tasks and volitional human motions. The approach in [9] is designed specifically for forward leaning, failing to accommodate various ways a human can fall. The generated trajectory can also be overly constraining an individual's voluntary motion. While [10] requires limited subject-specific customization, the pre-defined assistive torques do not take into account each user's volitional motion when reacting to a fall. Similarly, the kinematics-based controller in [11] aims to restore human joints to pre-defined equilibrium positions, ignoring the dynamic nature of joint motions during foot slips. When recovering from loss of balance or a potential fall, it is crucial to consider volitional human behaviors when designing assistive strategies, rather than restricting joint movements to normative trajectories.

To design balance recovery strategies without enforcing kinematic trajectories, we need to first identify indicators that can reflect ambulatory balance. Various approaches such as maximum Lyapunov exponent, long-range correlations, variability measures, and extrapolated center of mass (XCoM) [12] have been proposed to indicate balance. During human locomotion, the level of stability will decrease during single support phase as the body needs to fall forward to ambulate. The swing leg needs to prepare to catch the falling body at the onset of the next step [13]. Prior research shows that the Center of Mass (CoM) during walking serves as a measure for evaluating balance [14], and the capacity to position the foot correctly to manage CoM position is an important skill to maintain balance. We therefore choose CoM to define our safety indicator because of its feasibility and simplicity in real-time implementation. On the other hand, control barrier func-

tions (CBFs) have been prevalent in designing controllers that force the system to approach a pre-specified safe set [15]. CBF has been used in research areas where safety is critical, such as adaptive cruise control [16], dynamic balancing on Segway type robot [17], and multi-agent systems [18]. Predominantly, CBF has been applied to achieve stable walking gait for exoskeletons on level-ground [19] or bipeds on stepping stones [20] given its low computation cost in real time [21]. Defining CBF based on CoM has the potential to rapidly facilitate safe control strategies to mitigate the loss of balance during human locomotion. To consider a human's volitional motion when reacting to a fall, it is essential to estimate human joint torques. Nonlinear disturbance observers (NDOs) have been applied to robots for estimating disturbance terms in dynamics using angular information [22]. Since human joint torques can also be treated as the "disturbance term" in dynamics, we can use NDO to estimate human torques.

In this letter, we propose a framework to augment safety of human volitional motion during locomotion via exoskeletons. The contributions of this letter are:

1) We develop a safety framework for balance recovery considering human inputs, evaluating CoM positioning and early foot strikes to define independent safety indicators (thus CBFs) not reliant on reference trajectories.
2) We propose using a double-layer Quadratic Program (QP) structure with a human-centric weight matrix in the cost functions to determine the control law. The weight matrix will adapt dynamically to human motions, minimizing interference with natural behaviors.
3) We modified a traditional NDO to estimate human joint torques and external forces.

II. Preliminaries

A. Dynamics of Human and Exoskeleton Model

We model a human wearing an exoskeleton as a rigid sagittal-plane biped because human walking is primarily a sagittal-plane task [23]. The Euler-Lagrange dynamics of the human-exoskeleton system [24] can be expressed as

$$M\ddot{q} + C\dot{q} + N + A^T\lambda = \tau + J^T F_{\text{perturb}}, \tag{1}$$

where n is the degrees of freedom (DoFs), $M \in \mathbb{R}^{\text{n}\times\text{n}}$ is the inertia matrix, $C \in \mathbb{R}^{\text{n}\times\text{n}}$ is the Coriolis/centrifugal matrix, and $N \in \mathbb{R}^{\text{n}}$ indicates the gravitational forces. The inertial parameters within these matrices are the combined totals of both human and exoskeleton parameters. The constraint matrix A, defined as the gradient of holonomic constraint functions, maps the ground reaction forces (*i.e.*, Lagrange multiplier) $\lambda = \hat{\lambda} + \check{\lambda}\tau$ into the overall dynamics, where $\hat{\lambda} = W(\dot{A}\dot{q} - AM^{-1}N)$, $W = (AM^{-1}A^T)^{-1}$, and $\check{\lambda} = WAM^{-1}$ [24]. The overall internal torque τ consists of the human torque vector τ_{hum} and the exoskeleton torque vector $\tau_{\text{exo}} = Bu$, where $B = (0_{\text{p}\times(\text{n}-\text{p})},\ I_{\text{p}\times\text{p}})^T \in \mathbb{R}^{\text{n}\times\text{p}}$ maps the exoskeleton torque $u \in \mathbb{R}^{\text{p}}$ into the overall dynamics (p will be specified in Sec. IV-A). The vector $F_{\text{perturb}} \in \mathbb{R}^6$ summarizes all external perturbation forces and is projected into the overall dynamics via the Jacobian matrix $J \in \mathbb{R}^{6\times\text{n}}$. It is possible to estimate the interaction forces between the human and the exoskeleton [25], which can be included in τ.

B. Review of Control Barrier Functions

The general form of a nonlinear system can be expressed as:

$$\dot{x} = f(x) + g(x)u, \tag{2}$$

where $x \in \mathcal{D} \subset \mathbb{R}^{\text{n}}$ is the state vector, $f(x)$ and $g(x)$ are locally Lipschitz, and the control input $u \in \mathcal{U} \subset \mathbb{R}^{\text{m}}$. Note that (1) can be expressed in the form of (2) by choosing $x = [q^T, \dot{q}^T]^T \in \mathbb{R}^{2\text{n}}$, *i.e.*,

$$\dot{x} = f(x) + g(x)u = \begin{bmatrix} \dot{q} \\ M^{-1}Q \end{bmatrix} + \begin{bmatrix} 0 \\ M^{-1}B \end{bmatrix} u, \tag{3}$$

where $Q = -C\dot{q} - N - A^T\lambda + \tau_{\text{hum}} + J^T F_{\text{perturb}}$.

Define a closed set $\mathcal{C}$ that contains all admissible safe configurations with a continuously differentiable function $h(x) : \mathcal{D} \to \mathbb{R}$, *i.e.*, $\mathcal{C} = \{x \in \mathcal{D} \subset \mathbb{R}^{\text{n}} : h(x) \geq 0\}$, we can ensure safety by making it asymptotically stable and forward-invariant in $\mathcal{D}$. Assume h (with x omitted hereafter) has relative degree one, h is a CBF if there exists an extended class $\mathcal{K}_\infty$ function α such that for (2),

$$\sup_{u\in U}[L_f h + L_g h u] \geq -\alpha(h), \tag{4}$$

where $L_f h$ and $L_g h$ are Lie derivatives [26]. Any Lipschitz continuous controller u chosen from the set

$$K_{\text{cbf}}(x) = \{u \in \mathcal{U} : L_f h + L_g h u + \alpha(h) \geq 0\} \tag{5}$$

can render the set $\mathcal{C}$ safe and asymptotically stable in $\mathcal{D}$.

III. Safety Augmentation based on CBFs

In this section, we propose a framework for lower-limb exoskeletons to augment safety of human locomotion. In particular, we aim to restore balance considering volitional human inputs. The safety control strategies are generated from a double-layer QP structure with human preferences incorporated to determine user-friendly assistive strategies.

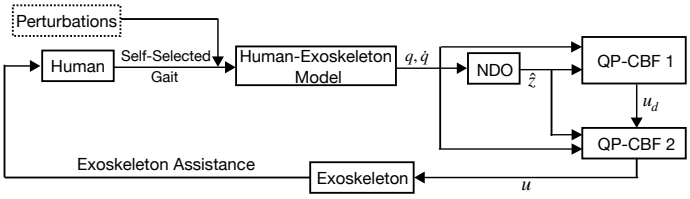

Figure 1. Overall diagram of the safety augmentation framework. The NDO and the term $\hat{z}$ will be specified in Sec. III-C.

A. CoM-Based Control Barrier Function Design

We first use a CoM-based function similar to XCoM to define CBFs. To accommodate cases where a human undergoes significant perturbation such that continued walking is not immediately feasible, we propose the following safety function

$$s_1 = (2\text{sig}(k_{\text{com}}(\text{CoM}_x - p_{\text{st,x}})) - 1)(p_{\text{sw,x}} - \text{CoM}_x) \geq 0, \tag{6}$$

where $p_{\text{st,x}}$ and $p_{\text{sw,x}}$ represent the horizontal positions of the stance and swing feet, respectively, and CoM_x indicates the horizontal position of the CoM. The function $\text{sig}(\cdot)$ is the sigmoid function, and k_{com} is a positive constant to control its steepness. In (6), the term $(p_{\text{sw,x}} - \text{CoM}_\text{x})$ dominates to render rapid movement of the swing leg (as opposed to the

stance leg) for regaining balance. In addition, early strikes at the point of minimum toe clearance increases the risk of falling from a trip [27] when trying to regain balance. We therefore define the second safety function to avoid early strike as

$$s_2 = p_{\text{sw,y}} - p_{\text{ground,y}} - c_{\text{clearance}} \geq 0, \tag{7}$$

where $p_{\text{ground,y}}$ is the ground height, and $c_{\text{clearance}}$ is a small positive number that guarantees the swing leg stays above the ground. Illustrations of both safety conditions are shown in Fig. 2. Finally, we define a relative-degree one CBF based on s_1 and s_2 as

$$h_i = \gamma_i s_i + \dot{s}_i + c_i, \quad i \in \{1,\ 2\}, \tag{8}$$

where c_i is a positive relaxation constant that allows the state to approach or slightly move outside the safe set, and $\gamma_i > 0$ adjusts the contribution of s_i and $\dot{s}_i$ to h_i [28]. In (8), we use a similar but different concept than XCoM, *i.e.*, $\text{CoM} + \dot{\text{CoM}}/\omega_0$, where ω_0 is the eigenfrequency [12], to provide more flexibility in parameter tuning.

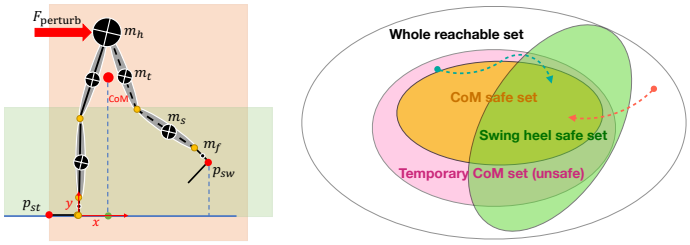

Figure 2. Left: Illustration of the safety conditions (6) (orange) and (7) (green). Solid and dashed lines represent stance and swing legs, and F_{perturb} denotes the perturbation force. The green dot is the projected position of the CoM onto the ground. Right: Illustration of safe sets with respect to h_1 (orange) and h_2 (green). Dashed lines are possible trajectories generated by control actions (12) and (14).

B. Control Structure

The major reason that we incorporate constraints in two separate QPs is to prioritize the tasks based on their urgency and to avoid infeasibilities in finding solutions. Since the control framework does not rely on pre-defined joint trajectories, the exoskeleton does not need to exactly follow the control torques with both constraints satisfied. Instead, the exoskeleton should be able to evaluate the situation to take the most appropriate action. When the swing foot clearance is large enough such that early foot strike is not a concern, balance recovery will be the major task. In contrast, when the swing heel is about to touch the ground before balance is regained, the objective of balance recovery can be relaxed for a short while to avoid early foot strikes. In this case, we should allow the system to temporarily deviate from the safe set defined by h_1 until the risk of early foot strike is resolved (Fig. 2). Satisfying both constraints within one QP could result in infeasibilities.

With h_i defined in (8), we can now incorporate it as a constraint in QPs. Conventional cost functions of QPs are usually in quadratic forms of actuator torques with pre-defined gain matrices [15], [28]. For assisting humans, cost function with pre-defined weights of actuator torques may result in undesirable assistance at certain joints. To make sure an exoskeleton has minimum interference on volitional human motion whilst still assisting a person, we first calculate the change rate of h_1 with human inputs only (*i.e.*, $u = 0$):

$$\dot{h}_{\text{hum}} = \frac{\partial h_1}{\partial q}\dot{q} + \frac{\partial h_1}{\partial \dot{q}} M^{-1} Q. \tag{9}$$

Since $\dot{h}_{\text{hum}}$ in (9) contains only the human inputs, it reflects the change of h_1 when only humans were reacting to an unsafe scenario. Equation (9) as well as other operations in terms of h_i throughout this section require the knowledge of human inputs and external perturbation forces. Estimation of their values will be introduced in Sec. III-C. Similar to (9), with actuators on, we have

$$\dot{h}_1 = \frac{\partial h_1}{\partial q}\dot{q} + \frac{\partial h_1}{\partial \dot{q}} M^{-1}(Q + Bu). \tag{10}$$

To ensure the exoskeleton assist humans with minimum interferences with their volitional motion, we want to minimize the difference between (9) and (10), *i.e.*,

$$(\dot{h}_1 - \dot{h}_{\text{hum}})^2 = (\frac{\partial h_1}{\partial \dot{q}} M^{-1} B u)^2 := u^T H_{\text{CoM}}(q,\ \dot{q}) u. \tag{11}$$

Note that (11) has the same form as $u^T H u$ with $H = H_{\text{CoM}}(q,\ \dot{q}) = (\frac{\partial h_1}{\partial \dot{q}} M^{-1} B)^T (\frac{\partial h_1}{\partial \dot{q}} M^{-1} B)$. Since components of $H_{\text{CoM}}(q,\ \dot{q})$ are time-varying and dynamics-based, they provide a time-varying, human-centric weight matrix that dynamically considers human dynamics in real time. The QP for determining the desired torque u_d can be then written as

$$\begin{aligned} \min_{u_d} \quad & u_d^T H_{\text{CoM}}(q,\ \dot{q}) u_d \\ \text{s.t.} \quad & L_f h_1 + L_g h_1 u_d \geq -\alpha_1(h_1), \end{aligned} \tag{12}$$

where $\alpha_1(\cdot)$ is an extended class $\mathcal{K}_\infty$ function. Since a rapid recovery is desirable when humans lose balance, and we want to allow a human's CoM to have the flexibility of slowly approaching the boundary of a safe set when safe, $\alpha_1(\cdot)$ is selected as

$$\alpha_1(h_1) = \begin{cases} log(h_1 + 1), & \text{if } h_1 \geq 0, \\ \beta_1 h_1^3 + h_1, & \text{if } h_1 < 0, \end{cases} \tag{13}$$

where β_1 is a positive number that controls the magnitude of $L_f h_1 + L_g h_1 u_d$ when the system is unsafe. Note that α_1 can have other forms as long as it qualifies as a class $\mathcal{K}_\infty$ function. Minimizing $u_d^T H_{\text{CoM}}(q,\ \dot{q}) u_d$ in (12) provides the capability to have control torques close to human inputs when possible, while the CBF constraint forces the control torques to render safety, even if they may not closely align with human inputs in some extreme situations. Once we obtain u_d from (12), we propose the second QP as

$$\begin{aligned} \min_{\mathbf{u}=[u^T,\ \delta]^T} \quad & ||\mathbf{u} - \mathbf{u_d}||_2^2 \\ \text{s.t.} \quad & L_f h_2 + L_g h_2 u \geq -\alpha_2(h_2) + \delta, \\ & u_{\min} \leq u \leq u_{\max}, \end{aligned} \tag{14}$$

where $\mathbf{u_d} = [u_d^T, 0]^T \in \mathbb{R}^{\text{p}+1}$, $\delta \in \mathbb{R}$ is a relaxation term to avoid infeasibilities, $\alpha_2(h_2) = \beta_2 h_2^3$ is an extended class $\mathcal{K}_\infty$ function with $\beta_2 > 0$, and $u_{\min} \in \mathbb{R}^p$ and $u_{\max} \in \mathbb{R}^p$ are lower and upper bounds of the control torques, respectively. In (14), u_d serves as a reference for u. One potential challenge

of using a two-QP structure instead of a one-QP structure is the increased computational complexity. The time complexity of calculating (12) and (14) is $O(n^3 log(n))$ with matrix inverse, which is feasible for real-time implementations on a microprocessor in similar studies [29].

C. Modified Nonlinear Disturbance Observer

Different from control paradigms that do not consider human inputs, the proposed approach requires the information of volitional human motion to compute control laws u_d and u. Therefore, we modify an existing model-based NDO [22] to estimate human joint torques using only angular information [30]. Let $B_\lambda = B - A^T \check{\lambda}$, $\tilde{\tau}_{\rm hum} = (I - A^T \check{\lambda})\tau_{\rm hum}$, and define $z = M^{-1}(\tilde{\tau}_{\rm hum} + J^T F_{\rm perturb})$ as the term to be estimated, left-multiplying M^{-1} at both sides of (1), we have

$$z = \ddot{q} + M^{-1}C\dot{q} + M^{-1}N + M^{-1}A^T\hat{\lambda} - M^{-1}B_\lambda u. \quad (15)$$

Denoting $\hat{z}$ as the estimate for z and $e = z - \hat{z}$ as the estimation error, we have [22]:

$$\dot{\hat{z}} = Le = L(z - \hat{z}), \quad (16)$$

where $L \in \mathbb{R}^{\rm n \times n}$ is a positive-definite, diagonal matrix that can be designed to ensure fast convergence of e [22], where

$$\dot{e} = \dot{z} - \dot{\hat{z}} = \dot{z} - Le, \quad (17)$$

and e can be ensured to be uniformly ultimately bounded with selected parameters [30]. When external perturbations occur, (16) will estimate it as part of the "human torque". This is desirable for the control objective, as the knowledge of overall forces are required to solve (12) and (14). Note that in (16), we estimate the modified term $M^{-1}(\tilde{\tau}_{\rm hum} + J^T F_{\rm perturb})$ instead of the actual human input and external forces $\tilde{\tau}_{\rm hum} + J^T F_{\rm perturb}$. Due to the human-exoskeleton model used in this letter, the matrix M has some very small eigenvalues. Estimating $\tilde{\tau}_{\rm hum} + J^T F_{\rm perturb}$ directly will result in large estimation error when calculating $\ddot{q} = M^{-1}(-C\dot{q} - N - A^T\lambda + \tau + J^T F_{\rm perturb})$, which is the major usage of the NDO, even if the estimation error of $\tilde{\tau}_{\rm hum} + J^T F_{\rm perturb}$ is small.

IV. Simulations and Results

In this section, we present simulation results of a human wearing an exoskeleton (modeled as a biped) trying to restore balance under two conditions: recovery from a force perturbation (RP) applied on the hip joint during normal walking, and recovery from unsafe postures (RU), where the human starts from an initial posture that will lead to a fall.

A. Simulation Model

According to [31], stable dynamic gaits can be achieved on a seven-link biped with impedance control at each joint. The configuration vector of the simulation model (Fig. 2, left) is given as $q_{\rm sim} = (\mathrm{x}, \mathrm{y}, \phi, \theta_{\rm a}, \theta_{\rm k}, \theta_{\rm h}, \theta_{\rm sk}, \theta_{\rm sa})^T \in \mathbb{R}^8$, where (x, y) is the Cartesian coordinates of the heel, θ_i, $i \in \{\mathrm{a}, \mathrm{k}, \mathrm{h}, \mathrm{sk}, \mathrm{sa}\}$ indicates the relative angle of ankle, knee, hip, swing knee, and swing ankle, respectively. Each of these joints is actuated by an exoskeleton actuator, *i.e.*, $u = \{u_{\rm a}, u_{\rm k}, u_{\rm h}, u_{\rm sk}, u_{\rm sa}\} \in \mathbb{R}^5$. All these joints are also actuated by the human joint torque vector $\tau_{\rm hum} = -K_{\rm p}^v(q_{\rm sim} - \bar{q}_{\rm sim}) - K_{\rm d}^v \dot{q}_{\rm sim}$ with positive-definite gain matrices $K_{\rm p}^v$ and $K_{\rm d}^v$ and $\bar{q}_{\rm sim}$ as equilibrium positions. We first tuned gain matrices by trial and error to find a stable passive gait and then implemented the proposed control. All simulation parameters can be found in Table II of [32].

B. Results and Discussions

For the RP case, the biped started walking from a safe posture where its CoM stayed between the stance and swing legs. A horizontal perturbation force was applied on the hip joint between 0.06s and 0.065s. This case was simulated to verify if the proposed control paradigm will be triggered only when the safe conditions are violated and do not intervene with nominal human behaviors otherwise. For the RU case, the biped started from an initial posture that will lead to a fall if no control actions are applied.

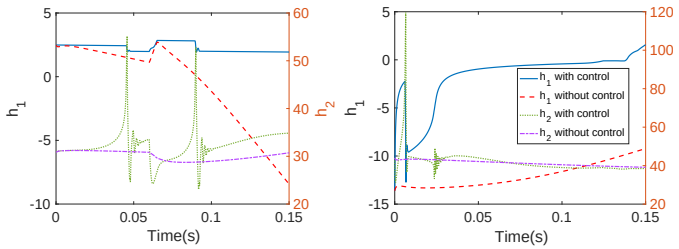

Figure 3. Values of h_1 and h_2 for RP (left) and RU (right). Balance during walking (*i.e.*, safety boundary) is primarily indicated by $h_1 = 0$.

We chose parameters $k_{\rm com} = 10$, $\gamma_1 = 30$, $c_1 = 0$, $\gamma_2 = 20$, $c_2 = 30$, $\beta_1 = 0.4$, and $\beta_2 = 1$ for RP with $F_{\rm perturb} = (3 \times 10^3, 0_{1\times 5})^T$N. The magnitude of perturbation was determined such that $\tau_{\rm hum}$ itself is insufficient in maintaining balance. For RU, we selected the parameters $k_{\rm com} = 7$, $\gamma_1 = 60$, $c_1 = 0$, $\gamma_2 = 30$, $c_2 = 50$, $\beta_1 = 15$, and $\beta_2 = 10$. The weight for relaxation term δ was selected to be 100 for both cases. We selected distinct parameters for each case based on differing priorities. In RP, we weight more on changes in CoM's velocity, whereas in RU, the position of CoM is the key to balance recovery from unsafe postures. We saturated exoskeleton torques at $\pm$ 700 Nm and $\pm$ 2×10^3 Nm for RP and RU, respectively.

The simulation results are shown in Figs. 3 to 7. Fig. 3 shows the value of safety functions with/without the safety controller. We can see that the human-exoskeleton system lost balance without the proposed safety control, while balance can be assured when safety control was employed. Fig. 4 illustrates the safety control torques and the ratios between human and exoskeleton torques. The exoskeleton generated almost zero torques before perturbation occurred and reacted instantaneously upon its occurrence. Spikes in exoskeleton torques are due to two reasons. Firstly, human input takes the form of an impedance controller with fixed equilibrium positions, which will resist any exoskeleton torques that drive human joints away from these equilibria, even if such torques were intended to ensure safety. Therefore, exoskeleton torques need to be sufficiently large to counteract human torque first to ensure safety. This phenomenon will be alleviated in practice with human volitional motion that do not track set points. Secondly, to render postures that violate safety, the applied perturbation needs to be sufficiently large to overcome

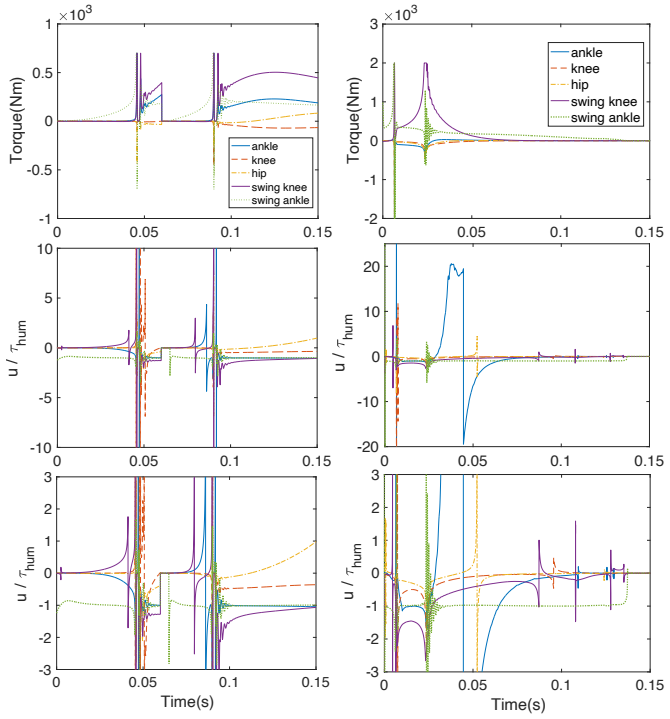

Figure 4. From top to bottom: control torques, ratio between control and human torques, and the zoomed version (left: RP; right: RU).

human joint torques, which also contributes to the spike in control torques. For example, the simulated human knee torque reached 1.2×10^4 Nm, which is much larger than biological torque of 199.8 ± 47.3 Nm (extensors) and 89.8 ± 21.0 Nm (flexors) [33]. To demonstrate that the proposed approach is feasible to be implemented, we plotted safety control torques offline in Fig. 5 using normative joint kinematics [34] with added deviation in orientation angle ($\pi/2$) and velocity ($\pi/3$ rad/s) to mimic unsafe cases. The resulting torques are not precise representations of real assistance but fall within an achievable range for current exoskeletons.

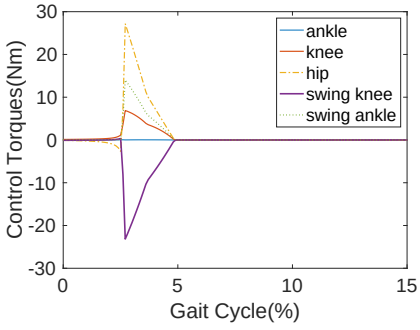

Figure 5. Control torques calculated using normative joint kinematics with added deviation on thigh angle and velocity at the beginning of a step.

In practice, the control framework is designed to provide partial assistance for humans. Balance will be regained as a consequence of joint efforts from both the human and the exoskeleton. The conducted simulation aims to demonstrate the capability of the control framework in extreme situations. Moreover, $\partial h_i/\partial q$ stayed non-zero during simulation, which numerically verifies the forward invariance of their corresponding CBF [26]. We also conducted simulations with one-QP structure that included both constraints with carefully tuned weights. However, simulations terminated due to infeasibilities in finding solutions. We further enforced zero torques at these infeasible points to proceed in simulation, and the results are similar to the ones of the two-QP structure (Fig. 6).

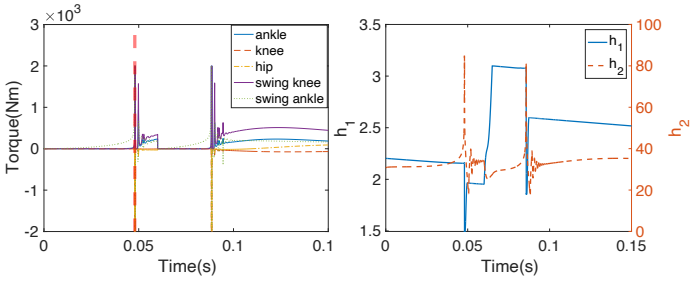

Figure 6. Control torques of one-QP structure for RP (left) and the associated safety functions (right). The red vertical line in the left graph indicates the first infeasible point, and torques were set to zeros hereafter for all infeasible points.

We plotted the screenshots of simulation animation in Fig. 7. The human-exoskeleton system was not able to maintain or restore balance with only τ_{hum}. When safety control was employed, the human-exoskeleton system can regain balance within a short period of time. In addition, in the RP case (left two rows), before perturbation was applied, the human-exoskeleton system had very similar walking patterns with and without safety control, indicating that the proposed method does not interfere with a human user's regular gait patterns. In the RU case, the human-exoskeleton system attempted to restore balance without the safety controller but was unsuccessful. On the other hand, using the proposed controller ensured safety and led to a posture similar to the unsafe one caused solely by human torques. This indicates that the time-varying weight matrix in (11) can be used to capture the human user's volitional motion.

Finally, to demonstrate robustness, we compared the gait sensitivity norm (GSN) $||\partial g/\partial r||_2$ [35] with and without the proposed safety control, where g is the gait indicator, and r is the input perturbation. A larger value of reciprocal GSN indicates stronger robustness. The perturbation was chosen to be a 100 N horizontal force with 60 ms duration applied on the hip joint at the beginning of a step. We activated the safety controller at the start and end of each step to prevent imbalanced postures and irregular step lengths, then computed the GSN at each heel strike across five steps. The system without/with safety control has a sum of reciprocal norm $1/||\partial g/\partial r||_2 = 2529.3$ and $1/||\partial g/\partial r||_2 = 5345.5$, respectively, indicating potential robustness of the proposed controller in restoring balance under perturbations. The associated exoskeleton torques were less than 50 Nm throughout the simulation, which are possible to be implemented.

V. Conclusion

We proposed a safety augmentation framework for exoskeletons based on a two-layer QP structure, with a particular case study on balance recovery. The safety indicators were defined based on human's CoM position and the swing foot clearance

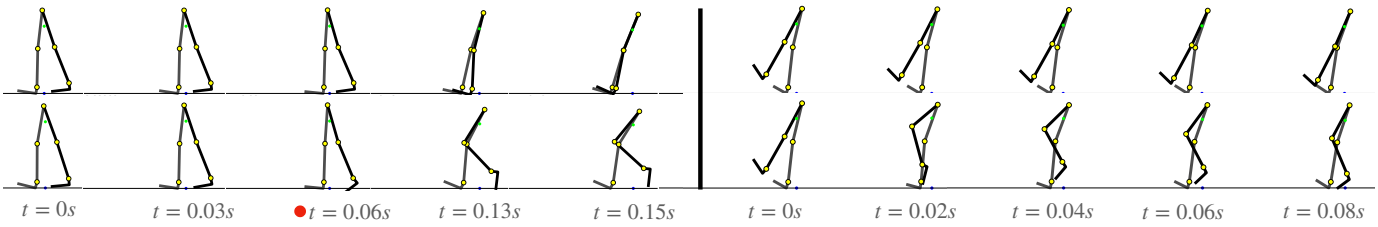

Figure 7. Left (RP)/right (RU): without (top)/with (bottom) safety control. The green and blue dots represent the human-exoskeleton system's CoM and its projection, respectively, and the red dot denotes the onset of perturbation. The animation video is available at https://www.youtube.com/watch?v=rZyEZS74eD0.

instead of pre-defined, safe trajectories. Two CBFs were then defined and incorporated as constraints in a two-layer QP structure to solve for the exoskeleton control law. An NDO was used to estimate human joint torques that were fitted into the overall control structure. Simulation results showed that a human user can maintain balance when undergoing gait perturbation, as well as restore balance from an initial unsafe posture with the help of the proposed safety control. Future work includes adding model predictive control components to the overall framework and experimental validations.

REFERENCES

[1] B. Moreland, R. Kakara, and A. Henry, "Trends in nonfatal falls and fall-related injuries among adults aged $\geq$ 65 years—united states, 2012–2018," *Morb Mortal Wkly Rep*, vol. 69, no. 27, p. 875, 2020.

[2] A. B. Peterson, "Deaths from fall-related traumatic brain injury—united states, 2008–2017," *Morb Mortal Wkly Rep*, vol. 69, 2020.

[3] H. Bateni and B. E. Maki, "Assistive devices for balance and mobility: benefits, demands, and adverse consequences," *Arch. Phys. M.*, vol. 86, no. 1, pp. 134–145, 2005.

[4] R. Baud, A. R. Manzoori, A. Ijspeert, and M. Bouri, "Review of control strategies for lower-limb exoskeletons to assist gait," *J Neuroeng Rehabil*, vol. 18, no. 1, pp. 1–34, 2021.

[5] T. Wang, Y. Zhu, T. Zheng, D. Sui, S. Zhao, and J. Zhao, "Palexo: A parallel actuated lower limb exoskeleton for high-load carrying," *IEEE Access*, vol. 8, pp. 67 250–67 262, 2020.

[6] Y. Ding, M. Kim, S. Kuindersma, and C. J. Walsh, "Human-in-the-loop optimization of hip assistance with a soft exosuit during walking," *Sci. Rob.*, vol. 3, no. 15, p. eaar5438, 2018.

[7] B. Johnson and M. Goldfarb, "A preliminary study on the feasibility of using a knee exoskeleton to reduce crouch gait in an adult with cerebral palsy," in *Int. Conf. Biomed. Robot. Biomechatronics*. IEEE, 2020, pp. 48–53.

[8] J. Pratt, J. Carff, S. Drakunov, and A. Goswami, "Capture point: A step toward humanoid push recovery," in *IEEE-RAS Int. Conf. Humanoid Robots*, 2006, pp. 200–207.

[9] M. Deng, Z. Ma, Y. Wang, H. Wang, Y. Zhao, Q. Wei, W. Yang, and C. Yang, "Fall preventive gait trajectory planning of a lower limb rehabilitation exoskeleton based on capture point theory," *Front. Inf. Technol. Electron. Eng.*, vol. 20, pp. 1322–1330, 2019.

[10] V. Monaco, P. Tropea, F. Aprigliano, D. Martelli, A. Parri, M. Cortese, R. Molino-Lova, N. Vitiello, and S. Micera, "An ecologically-controlled exoskeleton can improve balance recovery after slippage," *Sci. Rep.*, vol. 7, no. 1, p. 46721, 2017.

[11] C. Zhu and J. Yi, "Knee exoskeleton-enabled balance control of human walking gait with unexpected foot slip," *Robot. Autom. Lett.*, vol. 8, no. 11, pp. 7751–7758, 2023.

[12] S. M. Bruijn, O. Meijer, P. Beek, and J. H. van Dieen, "Assessing the stability of human locomotion: a review of current measures," *J. R. Soc. Interface*, vol. 10, no. 83, p. 20120999, 2013.

[13] M. Jacquelin Perry, "Gait analysis: normal and pathological function," *New Jersey: SLACK*, 2010.

[14] V. Lugade, V. Lin, and L.-S. Chou, "Center of mass and base of support interaction during gait," *Gait Posture*, vol. 33, no. 3, pp. 406–411, 2011.

[15] A. D. Ames, X. Xu, J. W. Grizzle, and P. Tabuada, "Control barrier function based quadratic programs for safety critical systems," *IEEE Trans. Autom. Control*, vol. 62, no. 8, pp. 3861–3876, 2016.

[16] A. D. Ames and M. Powell, "Towards the unification of locomotion and manipulation through control lyapunov functions and quadratic programs," in *Control of Cyber-Physical Systems: Workshop held at Johns Hopkins University*. Springer, 2013, pp. 219–240.

[17] T. Gurriet, A. Singletary, J. Reher, L. Ciarletta, E. Feron, and A. Ames, "Towards a framework for realizable safety critical control through active set invariance," in *IEEE Int. Conf. Cyber-Phys. Syst.*, 2018, pp. 98–106.

[18] U. Borrmann, L. Wang, A. D. Ames, and M. Egerstedt, "Control barrier certificates for safe swarm behavior," *IFAC-PapersOnLine*, vol. 48, no. 27, pp. 68–73, 2015.

[19] A. Agrawal and K. Sreenath, "Discrete control barrier functions for safety-critical control of discrete systems with application to bipedal robot navigation." in *Robotics: Science and Systems*, vol. 13. Cambridge, MA, USA, 2017, pp. 1–10.

[20] Q. Nguyen, A. Hereid, J. W. Grizzle, A. D. Ames, and K. Sreenath, "3D dynamic walking on stepping stones with control barrier functions," in *Conf. Decis. Control*. IEEE, 2016, pp. 827–834.

[21] Z. Li, "Comparison between safety methods control barrier function vs. reachability analysis," *arXiv preprint arXiv:2106.13176*, 2021.

[22] A. Mohammadi, M. Tavakoli, H. J. Marquez, and F. Hashemzadeh, "Nonlinear disturbance observer design for robotic manipulators," *Control Engineering Practice*, vol. 21, no. 3, pp. 253–267, 2013.

[23] M. Q. Liu, F. C. Anderson, M. G. Pandy, and S. L. Delp, "Muscles that support the body also modulate forward progression during walking," *J. Biomech.*, vol. 39, no. 14, pp. 2623–2630, 2006.

[24] R. M. Murray, Z. Li, and S. S. Sastry, *A Mathematical Introduction to Robotic Manipulation*. NW Boca Raton, FL: CRC press, 2017.

[25] M. Shushtari and A. Arami, "Human–exoskeleton interaction force estimation in indego exoskeleton," *Robotics*, vol. 12, no. 3, p. 66, 2023.

[26] A. D. Ames, S. Coogan, M. Egerstedt, G. Notomista, K. Sreenath, and P. Tabuada, "Control barrier functions: Theory and Applications," in *European Control Conference*. IEEE, 2019, pp. 3420–3431.

[27] B. W. Schulz, J. D. Lloyd, and W. E. Lee III, "The effects of everyday concurrent tasks on overground minimum toe clearance and gait parameters," *Gait Posture*, vol. 32, no. 1, pp. 18–22, 2010.

[28] Q. Nguyen and K. Sreenath, "Safety-critical control for dynamical bipedal walking with precise footstep placement," *IFAC-PapersOnLine*, vol. 48, no. 27, pp. 147–154, 2015.

[29] S. Trimble, W. Naeem, S. McLoone, and P. Sopasakis, "Context-aware robotic arm using fast embedded model predictive control," in *2020 31st Irish Signals and Systems Conference*. IEEE, 2020, pp. 1–6.

[30] M. Yu and G. Lv, "Task-invariant centroidal momentum shaping for lower-limb exoskeletons," in *Conf. Decis. Control*. IEEE, 2022, pp. 2054–2060.

[31] D. J. Braun, J. E. Mitchell, and M. Goldfarb, "Actuated dynamic walking in a seven-link biped robot," *IEEE/ASME Trans. Mechatron.*, vol. 17, no. 1, pp. 147–156, 2010.

[32] G. Lv, J. Lin, and R. D. Gregg, "Trajectory-free control of lower-limb exoskeletons through underactuated total energy shaping," *IEEE Access*, vol. 9, pp. 95 427–95 443, 2021.

[33] S. Barrué-Belou, M.-A. Démaret, A. Wurtz, A. Ducloux, F. Fourchet, and H. Bothorel, "Absolute and normalized normative torque values of knee extensors and flexors in healthy trained subjects: Asymmetry questions the classical use of uninjured limb as reference," *Arthrosc. Sports Med. Rehabil.*, vol. 6, no. 1, p. 100861, 2024.

[34] D. A. Winter, *Biomechanics and Motor Control of Human Movement*. John Wiley & Sons, 2009.

[35] D. G. Hobbelen and M. Wisse, "A disturbance rejection measure for limit cycle walkers: The gait sensitivity norm," *IEEE Trans. Robot.*, vol. 23, no. 6, pp. 1213–1224, 2007.